Harvesting mutual information from BTZ black hole spacetime

Kendra Bueley,[1,*] Luosi Huang,[1,†] Kensuke Gallock-Yoshimura,[1,‡] and Robert B. Mann[1,§]

[1] *Department of Physics and Astronomy, University of Waterloo, Waterloo, Ontario, N2L 3G1, Canada*

We investigate the correlation harvesting protocol for mutual information between two Unruh-DeWitt detectors in a static BTZ black hole spacetime. Here, the effects coming from communication and change in proper separation of the detectors are set to be negligible so that only a black hole affects the extracted mutual information. We find that, unlike the entanglement harvesting scenario, harvested mutual information is zero only when a detector reaches an event horizon, and that although the Hawking effect and gravitational redshift both affect the extraction of mutual information, it is extreme Hawking radiation that inhibits the detectors from harvesting.

arXiv:2205.07891v2 [quant-ph] 21 Jul 2022

I. INTRODUCTION

Relativistic quantum information theory studies the interplay between quantum information processing and relativistic effects, and has attracted much attention in recent years. Many of the studies use either the Bogoliubov transformation or particle detector models, such as Unruh-DeWitt (UDW) detectors [1, 2], to examine, for example, the quantum teleportation protocol [3, 4], relativistic quantum communication channels [5–8], and entanglement degradation [9, 10].

In particular the so-called *entanglement harvesting protocol* is an operation where multiple initially uncorrelated particle detectors extract entanglement from the vacuum of a quantum field via local interaction [11–13]. Entanglement harvesting exploits the fact that vacuum states of a quantum field are entangled [14, 15], and so even causally disconnected detectors can be correlated. Extensive research shows that the extracted entanglement is sensitive to spacetime properties [16–22] and the state of motion of the detectors [23–25].

Our particular interest lies in the impact of black holes on harvested correlations between detectors. The first investigation of the harvesting protocol in a black hole spacetime was done by Henderson *et al.* [19]. It was shown that there is an *entanglement shadow* — a region where two static detectors hovering outside a Bañados-Teitelboim-Zanelli (BTZ) black hole cannot harvest entanglement. This region is located near the black hole at sufficiently large angular separations of the detectors relative to the origin; it arises due to a combination of increased local Hawking temperature near the black hole and gravitational redshift suppression of nonlocal correlations. Other types of black holes have also been examined, including static detectors in Schwarzschild and Vaidya spacetimes [26], topological black holes [27], geons [28], corotating detectors around a rotating BTZ black hole [29], and freely falling detectors in Schwarzschild spacetime [30].

While most studies of the harvesting protocol focus on extraction of entanglement, little has been done for other correlations such as mutual information. Quantum mutual information quantifies the total amount of classical and quantum correlations including entanglement, and a few investigations of mutual information harvesting have been carried out [16, 31–33]. Unlike entanglement, mutual information does not vanish anywhere outside the event horizon, at least in $(1+1)$-dimensional settings [26, 30]. However a detailed study of how Hawking radiation and gravitational redshift influence the harvesting protocol for mutual information has not yet been carried out.

Our purpose here is to address this issue by examining the harvesting protocol for mutual information in the presence of a black hole. For simplicity, we consider the nonrotating BTZ black hole spacetime and, as with other studies [19], consider identical UDW detectors that are static outside of the horizon and do not communicate with each other [34]. This setup allows us to investigate effects that are purely due to the black hole, such as redshift and the Hawking effect. We obtain two key results. First, although the amount of harvested correlation is reduced by these effects as detectors get close to a black hole and vanishes at the event horizon, the "shadow" for mutual information is absent. Since entanglement cannot be harvested near a black hole, the extracted correlation is either classical or nondistillable entanglement. Second, the death of mutual information at the event horizon is due to Hawking radiation and not gravitational redshift.

Our paper is organized as follows. In Sec. II A we introduce the BTZ spacetime and the conformally coupled scalar field defined on this background. The final density matrix of UDW detectors after they interact with the quantum field is given in Sec. II B. The mutual information can be written in terms of elements in this density matrix. Then we show how mutual information is affected by the black hole in Sec. III, followed by conclusion in Sec. IV. Throughout this paper, we use the units $\hbar = c = 1$ and the signature $(-,+,+)$. Also, $\mathsf{x} := x^\mu$ denotes an event in coordinates x^μ.

* kbueley@uwaterloo.ca
† luosi.huang@uwaterloo.ca
‡ kgallock@uwaterloo.ca
§ rbmann@uwaterloo.ca

II. UDW DETECTORS IN BTZ SPACETIME

A. BTZ spacetime and quantum fields

The BTZ spacetime [35, 36] is a $(2+1)$-dimensional black hole spacetime with a negative constant curvature. Its line-element in static coordinates is given by

$$\mathrm{d}s^2 = -f(r)\mathrm{d}t^2 + \frac{\mathrm{d}r^2}{f(r)} + r^2\mathrm{d}\phi^2\,, \tag{1a}$$

$$f(r) = \frac{r^2}{\ell^2} - M\,, \tag{1b}$$

with $t \in \mathbb{R}, r \in (0,\infty)$, and $\phi \in [0, 2\pi)$. The dimensionless quantity M is the mass of the BTZ black hole and ℓ is known as the AdS length, which determines the negative curvature of the spacetime. The event horizon r_h of a nonrotating BTZ black hole can be obtained from the roots of $f(r) = 0$, which is

$$r_\mathrm{h} = \ell\sqrt{M}\,. \tag{2}$$

We will examine correlations between two detectors in terms of their proper distance. For $r_2 > r_1 \geq r_\mathrm{h}$, the proper distance, $d(r_1, r_2)$, between two spacetime points (t, r_1, ϕ) and (t, r_2, ϕ) is given by

$$d(r_1, r_2) = \ell \ln\left(\frac{r_2 + \sqrt{r_2^2 - r_\mathrm{h}^2}}{r_1 + \sqrt{r_1^2 - r_\mathrm{h}^2}}\right). \tag{3}$$

We will consider the case where detector A is closer to the event horizon, namely $r_\mathrm{B} > r_\mathrm{A} > r_\mathrm{h}$, and fix the proper separation between the detectors $d_\mathrm{AB} \coloneqq d(r_\mathrm{A}, r_\mathrm{B})$. We also write $d_j \coloneqq d(r_\mathrm{h}, r_j)$, $j \in \{\mathrm{A}, \mathrm{B}\}$ for simplicity.

The Hawking temperature T_H of a BTZ black hole is known to be[1] $T_\mathrm{H} = r_\mathrm{h}/2\pi\ell^2$ and the local temperature T_j at radial position $r = r_j$ is given by

$$T_j = \frac{T_\mathrm{H}}{\gamma_j}\,, \tag{4}$$

where

$$\gamma_j = \frac{\sqrt{r_j^2 - r_\mathrm{h}^2}}{\ell} \qquad (r_j \geq r_\mathrm{h}) \tag{5}$$

is the redshift factor. For $r_\mathrm{B} > r_\mathrm{A} > r_\mathrm{h}$, the redshift factors for detectors A and B can be written in terms of the proper distances:

$$\gamma_\mathrm{A} = \frac{r_\mathrm{h}}{\ell}\sinh\frac{d_\mathrm{A}}{\ell}\,, \tag{6a}$$

$$\gamma_\mathrm{B} = \frac{r_\mathrm{h}}{\ell}\sinh\frac{d_\mathrm{AB} + d_\mathrm{A}}{\ell}\,. \tag{6b}$$

[1] Note that $T_\mathrm{H} \propto \sqrt{M}$ in contrast to the $T_\mathrm{H} \propto 1/M$ behavior for a Schwarzschild black hole.

More precisely, the temperature (4) is known as the Kubo-Martin-Schwinger (KMS) temperature at $r = r_j$.

We now introduce a conformally coupled quantum scalar field $\hat{\phi}(\mathsf{x})$ in the BTZ spacetime. Choosing the Hartle-Hawking vacuum $|0\rangle$, the Wightman function $W_\mathrm{BTZ}(\mathsf{x}, \mathsf{x}') \coloneqq \langle 0|\,\hat{\phi}(\mathsf{x})\hat{\phi}(\mathsf{x}')\,|0\rangle$ can be constructed from the image sum of the Wightman function in the AdS_3 spacetime, $W_\mathrm{AdS}(\mathsf{x}, \mathsf{x}')$ [37]. Let $\Gamma : (t, r, \phi) \to (t, r, \phi + 2\pi)$ represent the identification of a point x in AdS_3 spacetime. Then W_BTZ is known to be

$$\begin{aligned} W_\mathrm{BTZ}(\mathsf{x}, \mathsf{x}') &= \sum_{n=-\infty}^{\infty} W_\mathrm{AdS}(\mathsf{x}, \Gamma^n\mathsf{x}') \\ &= \frac{1}{4\pi\sqrt{2}\ell}\sum_{n=-\infty}^{\infty}\left[\frac{1}{\sqrt{\sigma_\epsilon(\mathsf{x}, \Gamma^n\mathsf{x}')}} - \frac{\zeta}{\sqrt{\sigma_\epsilon(\mathsf{x}, \Gamma^n\mathsf{x}') + 2}}\right], \end{aligned} \tag{7}$$

where

$$\begin{aligned} \sigma_\epsilon(\mathsf{x}, \Gamma^n\mathsf{x}') = \frac{rr'}{r_\mathrm{h}^2}\cosh\left[\frac{r_\mathrm{h}}{\ell}(\Delta\phi - 2\pi n)\right] - 1 \\ - \frac{\sqrt{(r^2 - r_\mathrm{h}^2)(r'^2 - r_\mathrm{h}^2)}}{r_\mathrm{h}^2}\cosh\left(\frac{r_\mathrm{h}}{\ell^2}\Delta t - \mathrm{i}\epsilon\right) \end{aligned} \tag{8}$$

with $\Delta\phi \coloneqq \phi - \phi'$, $\Delta t \coloneqq t - t'$, and ϵ is the ultraviolet regulator. $\zeta \in \{-1, 0, 1\}$ specifies the boundary condition for the field at the spatial infinity: Neumann $\zeta = -1$, transparent $\zeta = 0$, and Dirichlet $\zeta = 1$. We will choose $\zeta = 1$ throughout this article. We also note that $n = 0$ term in the Wightman function is called the AdS-Rindler term [38–40] , which corresponds to a uniformly accelerating detector in AdS_3 spacetime [41]; the remaining $(n \neq 0)$ terms are known as the BTZ terms, which yield the black hole contribution.

B. UDW detectors

A UDW detector is a two-level quantum system consisting of ground and excited states with energy gap Ω, and can be considered as a qubit. Let us prepare two pointlike UDW detectors A and B. Each of them has their own proper time τ_j ($j \in \{\mathrm{A}, \mathrm{B}\}$) and will interact with the local quantum field $\hat{\phi}(\mathsf{x})$ through the following interaction Hamiltonian

$$\hat{H}_j^{\tau_j}(\tau_j) = \lambda_j\chi_j(\tau_j)\hat{\mu}_j(\tau_j) \otimes \hat{\phi}(\mathsf{x}_j(\tau_j)),\ j \in \{\mathrm{A}, \mathrm{B}\} \tag{9}$$

in the interaction picture, where λ_j is the coupling strength and $\chi_j(\tau_j)$ is the switching function describing the interaction duration of detector-j. The operator $\hat{\mu}_j(\tau_j)$ is the so-called monopole moment, which describes the dynamics of a detector and is given by

$$\hat{\mu}_j(\tau_j) = |e_j\rangle\langle g_j|\,e^{\mathrm{i}\Omega_j\tau_j} + |g_j\rangle\langle e_j|\,e^{-\mathrm{i}\Omega_j\tau_j}, \tag{10}$$

where $|g_j\rangle, |e_j\rangle$, and Ω_j are respectively the ground, excited states of detector-j and the energy gap between

them. $\hat{\phi}(\mathsf{x}_j(\tau_j))$ is the pullback of the field operator along detector-j's trajectory. We put the superscript on the Hamiltonian $\hat{H}_j^{\tau_j}(\tau_j)$ to indicate that it is the generator of time-translation with respect to the proper time τ_j. In what follows, we assume that the detectors have the same coupling strength λ and energy gap Ω.

Let us write the total interaction Hamiltonian as a generator of time-translation with respect to the common time t in the BTZ spacetime:

$$\hat{H}_{\mathrm{I}}^t(t) = \frac{\mathrm{d}\tau_{\mathrm{A}}}{\mathrm{d}t}\hat{H}_{\mathrm{A}}^{\tau_{\mathrm{A}}}\big(\tau_{\mathrm{A}}(t)\big) + \frac{\mathrm{d}\tau_{\mathrm{B}}}{\mathrm{d}t}\hat{H}_{\mathrm{B}}^{\tau_{\mathrm{B}}}\big(\tau_{\mathrm{B}}(t)\big)\,, \tag{11}$$

so that the time-evolution operator $\hat{U}_{\mathrm{I}}$ is given by a time-ordering symbol $\mathcal{T}_t$ with respect to t [42, 43]:

$$\hat{U}_{\mathrm{I}} = \mathcal{T}_t \exp\left(-\mathsf{i}\int_{\mathbb{R}} \mathrm{d}t\, \hat{H}_{\mathrm{I}}^t(t)\right). \tag{12}$$

We now assume that the coupling strength λ is small and apply the Dyson series expansion to $\hat{U}_{\mathrm{I}}$:

$$\hat{U}_{\mathrm{I}} = \mathbb{1} + \hat{U}^{(1)} + \hat{U}^{(2)} + \mathcal{O}(\lambda^3)\,, \tag{13a}$$

$$\hat{U}^{(1)} = -\mathsf{i}\int_{-\infty}^{\infty} \mathrm{d}t\, \hat{H}_{\mathrm{I}}^t(t)\,, \tag{13b}$$

$$\hat{U}^{(2)} = -\int_{-\infty}^{\infty}\mathrm{d}t_1 \int_{-\infty}^{t_1}\mathrm{d}t_2\, \hat{H}_{\mathrm{I}}^t(t_1)\hat{H}_{\mathrm{I}}^t(t_2)\,. \tag{13c}$$

We further assume that the detectors and the field are initially in their ground states and uncorrelated. The initial state ρ_0 of the total system is then

$$\rho_0 = |g_{\mathrm{A}}\rangle\langle g_{\mathrm{A}}| \otimes |g_{\mathrm{B}}\rangle\langle g_{\mathrm{B}}| \otimes |0\rangle\langle 0|\,, \tag{14}$$

where $|0\rangle$ is the vacuum state of the field. After the interaction, the final total density matrix ρ_{tot} reads

$$\begin{aligned}\rho_{\mathrm{tot}} &= \hat{U}_{\mathrm{I}}\rho_0\hat{U}_{\mathrm{I}}^\dagger \\ &= \rho_0 + \rho^{(1,1)} + \rho^{(2,0)} + \rho^{(0,2)} + \mathcal{O}(\lambda^4),\end{aligned} \tag{15}$$

where $\rho^{(i,j)} = \hat{U}^{(i)}\rho_0\hat{U}^{(j)\dagger}$ and we used the fact that all the odd-power terms of λ vanish [16].

The final density matrix $\rho_{\mathrm{AB}} = \mathrm{Tr}_\phi[\rho_{\mathrm{tot}}]$ of the detectors in the basis $\{|g_{\mathrm{A}}g_{\mathrm{B}}\rangle, |g_{\mathrm{A}}e_{\mathrm{B}}\rangle, |e_{\mathrm{A}}g_{\mathrm{B}}\rangle, |e_{\mathrm{A}}e_{\mathrm{B}}\rangle\}$ is known to be

$$\rho_{\mathrm{AB}} = \begin{bmatrix} 1-\mathcal{L}_{\mathrm{AA}}-\mathcal{L}_{\mathrm{BB}} & 0 & 0 & \mathcal{M}^* \\ 0 & \mathcal{L}_{\mathrm{BB}} & \mathcal{L}_{\mathrm{AB}}^* & 0 \\ 0 & \mathcal{L}_{\mathrm{AB}} & \mathcal{L}_{\mathrm{AA}} & 0 \\ \mathcal{M} & 0 & 0 & 0 \end{bmatrix} + \mathcal{O}(\lambda^4)\,, \tag{16}$$

where

$$\begin{aligned}\mathcal{L}_{ij} = \lambda^2 \int_{\mathbb{R}}\mathrm{d}\tau_i \int_{\mathbb{R}}\mathrm{d}\tau_j'\, \chi_i(\tau_i)\chi_j(\tau_j')e^{-\mathsf{i}\Omega(\tau_i-\tau_j')} \\ \times W_{\mathrm{BTZ}}\big(\mathsf{x}_i(\tau_i),\mathsf{x}_j(\tau_j')\big)\,,\end{aligned} \tag{17}$$

$$\begin{aligned}\mathcal{M} = -\lambda^2 \int_{\mathbb{R}}\mathrm{d}\tau_{\mathrm{A}} \int_{\mathbb{R}}\mathrm{d}\tau_{\mathrm{B}}\, \chi_{\mathrm{A}}(\tau_{\mathrm{A}})\chi_{\mathrm{B}}(\tau_{\mathrm{B}})e^{\mathsf{i}\Omega(\tau_{\mathrm{A}}+\tau_{\mathrm{B}})} \\ \times \big[\Theta\big(t(\tau_{\mathrm{A}})-t(\tau_{\mathrm{B}})\big)W_{\mathrm{BTZ}}\big(\mathsf{x}_{\mathrm{A}}(\tau_{\mathrm{A}}),\mathsf{x}_{\mathrm{B}}(\tau_{\mathrm{B}})\big) \\ + \Theta\big(t(\tau_{\mathrm{B}})-t(\tau_{\mathrm{A}})\big)W_{\mathrm{BTZ}}\big(\mathsf{x}_{\mathrm{B}}(\tau_{\mathrm{B}}),\mathsf{x}_{\mathrm{A}}(\tau_{\mathrm{A}})\big)\big]\,,\end{aligned} \tag{18}$$

where $\Theta(t)$ is the Heaviside step function. The off-diagonal elements $\mathcal{M}$ and $\mathcal{L}_{\mathrm{AB}}$ are responsible for entanglement and mutual information, respectively. It is worth knowing that the elements satisfy $\mathcal{L}_{\mathrm{AA}}\mathcal{L}_{\mathrm{BB}} \geq |\mathcal{L}_{\mathrm{AB}}|^2$ [17].

The total classical and quantum correlations are given by

$$\begin{aligned}I_{\mathrm{AB}} = \mathcal{L}_+\ln\mathcal{L}_+ + \mathcal{L}_-\ln\mathcal{L}_- \\ - \mathcal{L}_{\mathrm{AA}}\ln\mathcal{L}_{\mathrm{AA}} - \mathcal{L}_{\mathrm{BB}}\ln\mathcal{L}_{\mathrm{BB}} + \mathcal{O}(\lambda^4)\,,\end{aligned} \tag{19}$$

which is the mutual information I_{AB} between detectors A and B, where

$$\mathcal{L}_\pm \coloneqq \frac{1}{2}\left(\mathcal{L}_{\mathrm{AA}}+\mathcal{L}_{\mathrm{BB}} \pm \sqrt{(\mathcal{L}_{\mathrm{AA}}-\mathcal{L}_{\mathrm{BB}})^2+4|\mathcal{L}_{\mathrm{AB}}|^2}\right). \tag{20}$$

Note that $I_{\mathrm{AB}} = 0$ if $\mathcal{L}_{\mathrm{AB}} = 0$, and from the condition, $\mathcal{L}_{\mathrm{AA}}\mathcal{L}_{\mathrm{BB}} \geq |\mathcal{L}_{\mathrm{AB}}|^2$, we have $\mathcal{L}_{\mathrm{AA}}\mathcal{L}_{\mathrm{BB}} = 0 \Rightarrow |\mathcal{L}_{\mathrm{AB}}| = 0 \Rightarrow I_{\mathrm{AB}} = 0$.

We will use a Gaussian switching function with a typical interaction duration σ,

$$\chi_j(\tau_j) = e^{-\tau_j^2/2\sigma^2}, \tag{21}$$

in which case $\mathcal{L}_{ij}$ can be reduced to single integrals as shown in Appendix A.

III. RESULTS

In this section we investigate how a black hole affects the extraction of mutual information. Detectors A and B are both static outside the black hole and aligned along an axis through its center [so that $\Delta\phi = 0$ in (8)], and they switch at the same time. To see the effects purely coming from the black hole, we always fix the proper separation, d_{AB}, between A and B in such a way that the contribution from communication is negligible. In what follows we write quantities in units of the Gaussian width σ. For example, $\tilde{\lambda} \coloneqq \lambda\sqrt{\sigma}$ denotes a dimensionless coupling constant.

Let us first analyze the dependence on the energy gap Ω and the proper distance d_{A} between detector A and the event horizon in Fig. 1. We fix $\ell/\sigma = 10, M = 10^{-2}$ and $d_{\mathrm{AB}}/\sigma = 7$, and treat mutual information as a function of Ω and d_{A}: $I_{\mathrm{AB}} = I_{\mathrm{AB}}(\Omega, d_{\mathrm{A}})$. Figures 1(b) and (c) depict slices of (a) with constant d_{A}/σ and $\Omega\sigma$, respectively. From Figs. 1(a) and (b), one finds that there exists an optimal value of Ω to extract correlation for each d_{A}.

Figure 1(c) displays the dependence of mutual information on d_{A}. From Eqs. (4) and (6), the change in mutual information in this figure is caused by both particle production and redshift effects. Overall, as the detectors together move away from the black hole at constant

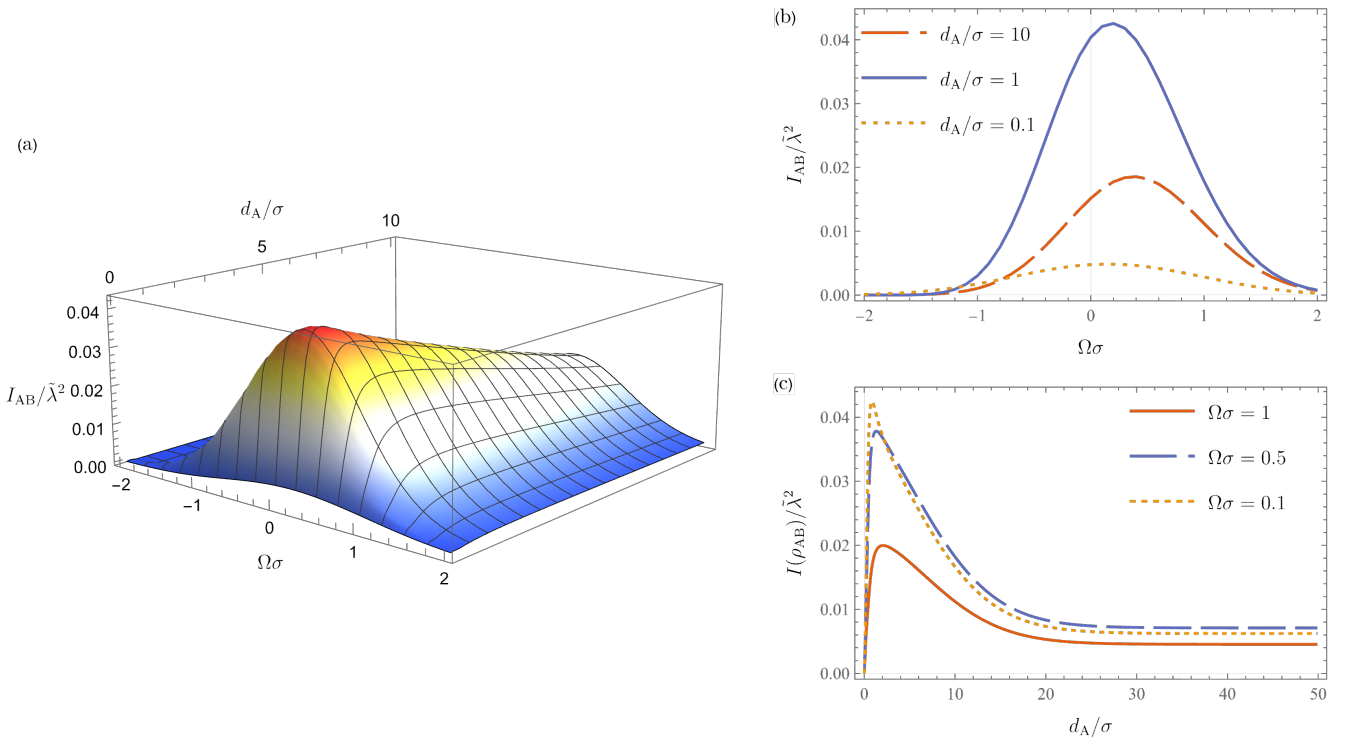


FIG. 1. (a) 3D plot of mutual information $I_{AB}/\tilde{\lambda}^2$ as a function of energy gap $\Omega\sigma$ and proper distance d_A/σ. Here, $\ell/\sigma = 10, M = 10^{-2}$, and $d_{AB}/\sigma = 7$. (b) Some slices of (a) with constant $d_A/\sigma = 10, 1$, and 0.1. (c) Slices of (a) with constant $\Omega\sigma = 1, 0.5$, and 0.1.

proper separation, the mutual information initially grows very quickly, reaches a maximum, and then flattens to a constant corresponding to detectors in AdS_3 spacetime.

Recall that a black hole inhibits static detectors from harvesting entanglement when one of them is close to the event horizon due to extreme Hawking radiation and redshift [19]. This region near the event horizon is called the "entanglement shadow." In contrast to this we see in Fig. 1(c) that mutual information is everywhere nonzero except at $d_A/\sigma = 0$. Thus harvested correlation in the entanglement shadow contains either classical correlation or nondistillable entanglement. These results are commensurate with previous studies in $(1+1)$ dimensions [26, 30], in which mutual information had no shadow region for all $\Omega\sigma$.

As suggested in Ref. [19], we expect that the decline of correlation near the event horizon and its death at $d_A/\sigma = 0$ are caused by the gravitational redshift and extreme Hawking radiation. From now on, we examine how these two effects contribute by treating detector A's redshift factor γ_A and KMS temperature T_A as independent variables, and write mutual information as a function of them: $I_{AB} = I_{AB}(T_A, \gamma_A)$. We will show that the decline of mutual information is caused by both high temperature and large redshift, but the death is purely due to an extreme temperature effect.

Our strategy is to use $I_{AB} = I_{AB}(T_A, \gamma_A)$ and fix either T_A or γ_A so that one can see respectively the influence of γ_A and T_A. To this end, one needs to write the event horizon r_h and the proper distance d_A in terms of T_A and γ_A:

$$r_h = 2\pi\ell^2 T_A \gamma_A \,, \tag{22}$$

$$d_A = \ell \ln \frac{1+\sqrt{1+(2\pi\ell T_A)^2}}{2\pi\ell T_A} \,. \tag{23}$$

Thus the scenario where $T_A = const$ is different from that of $\gamma_A = const$ as illustrated in Fig. 2. Fixing T_A and varying γ_A corresponds to a situation in Fig. 2(a-i) where the size of the black hole varies with γ_A and the proper distance d_A does not change. Note that the local temperature detected by detector B, T_B, is also fixed. Meanwhile, setting γ_A a constant and varying T_A means both r_h and d_A change with T_A as shown in Fig. 2(b-i).

Using the setup given above, let us take a look at the AdS-Rindler ($n = 0$) and BTZ ($n \neq 0$) contributions in the response function $\mathcal{L}_{AA}/\tilde{\lambda}^2$ and the off-diagonal element $\mathcal{L}_{AB}/\tilde{\lambda}^2$. Figures 2(a-ii) and (a-iii) are $\mathcal{L}_{AA}/\tilde{\lambda}^2$ and $\mathcal{L}_{AB}/\tilde{\lambda}^2$ when the local KMS temperature of detector-A is fixed. One can observe that the AdS-Rindler term in $\mathcal{L}_{AA}$ and $\mathcal{L}_{AB}$ is independent of γ_A, whereas the BTZ part is nonvanishing only when $\gamma_A \ll 1$. Hence, $\mathcal{L}_{ij} = \mathcal{L}_{ij}^{(n=0)} + \mathcal{L}_{ij}^{(n\neq 0)}$ is nonzero for all γ_A, indicating that mutual information will not vanish because of the gravitational redshift.

On the other hand, Figs. 2(b) depict the matrix elements $\mathcal{L}_{ij}$ when the redshift factor γ_A is fixed. We

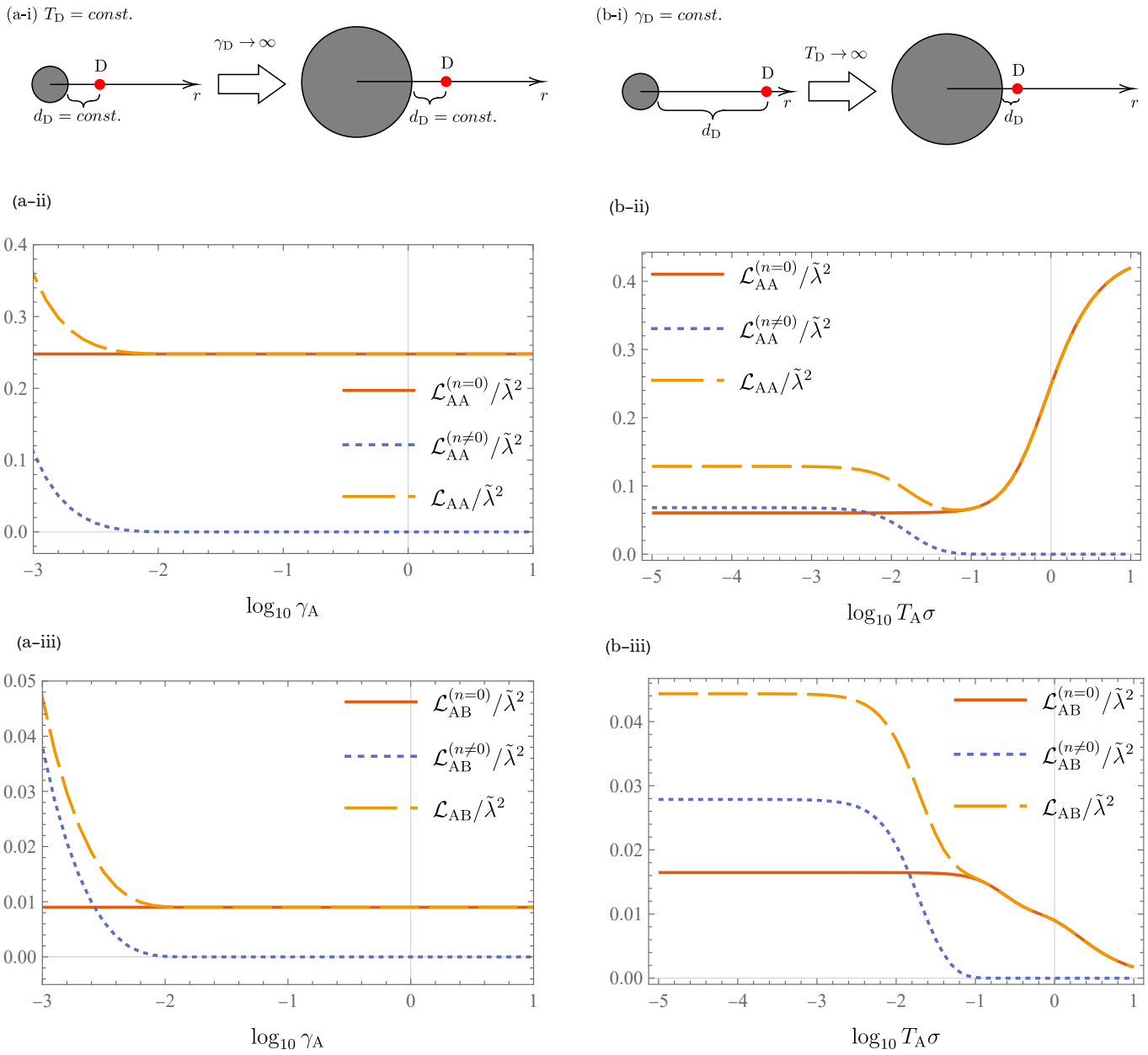


FIG. 2. AdS-Rindler and BTZ contributions in $\mathcal{L}_{ij}$. All figures have $\ell/\sigma = 10, d_{\rm A}/\sigma = 7$, and $\Omega\sigma = 1$. (a-i)-(a-iii): Varying $\gamma_{\rm A}$ while $T_{\rm A}\sigma = 1$ is fixed. For both $\mathcal{L}_{\rm AA}$ and $\mathcal{L}_{\rm AB}$, the AdS-Rindler part ($n = 0$) is independent of $\gamma_{\rm A}$ and the BTZ part ($n \neq 0$) is nonzero only for $\gamma_{\rm A} \ll 1$. Because of the AdS-Rindler contribution, the total $\mathcal{L}_{ij}$ is nonzero for all $\gamma_{\rm A}$. (b-i)-(b-iii): Varying $T_{\rm A}$ with fixed $\gamma_{\rm A} = 1/10$. For $\mathcal{L}_{\rm AB}$, both AdS-Rindler and BTZ terms vanish at high temperature.

first note that the response function $\mathcal{L}_{\rm AA}$ of detector A [Fig. 2(b-ii)] decreases as the temperature increases. In a nutshell, one expects the contrary: that a detector's response function increases monotonically as the local temperature increases. However, this turns out to be not necessarily true; even a carefully switched detector with an infinite interaction duration experiences "cool down" as temperature increases. More precisely, writing $\mathcal{F}(\Omega) = \mathcal{L}_{\rm DD}/\tilde{\lambda}^2$, the conditions

$$\frac{{\rm d}\mathcal{F}(\Omega)}{{\rm d}T_{\rm KMS}} < 0 \quad \text{weak} \tag{24}$$

$$\frac{\partial T_{\rm EDR}}{\partial T_{\rm KMS}} < 0 \quad \text{strong} \tag{25}$$

in the presence of a black hole are respectively referred to as the weak and strong anti-Hawking effects [38] (see

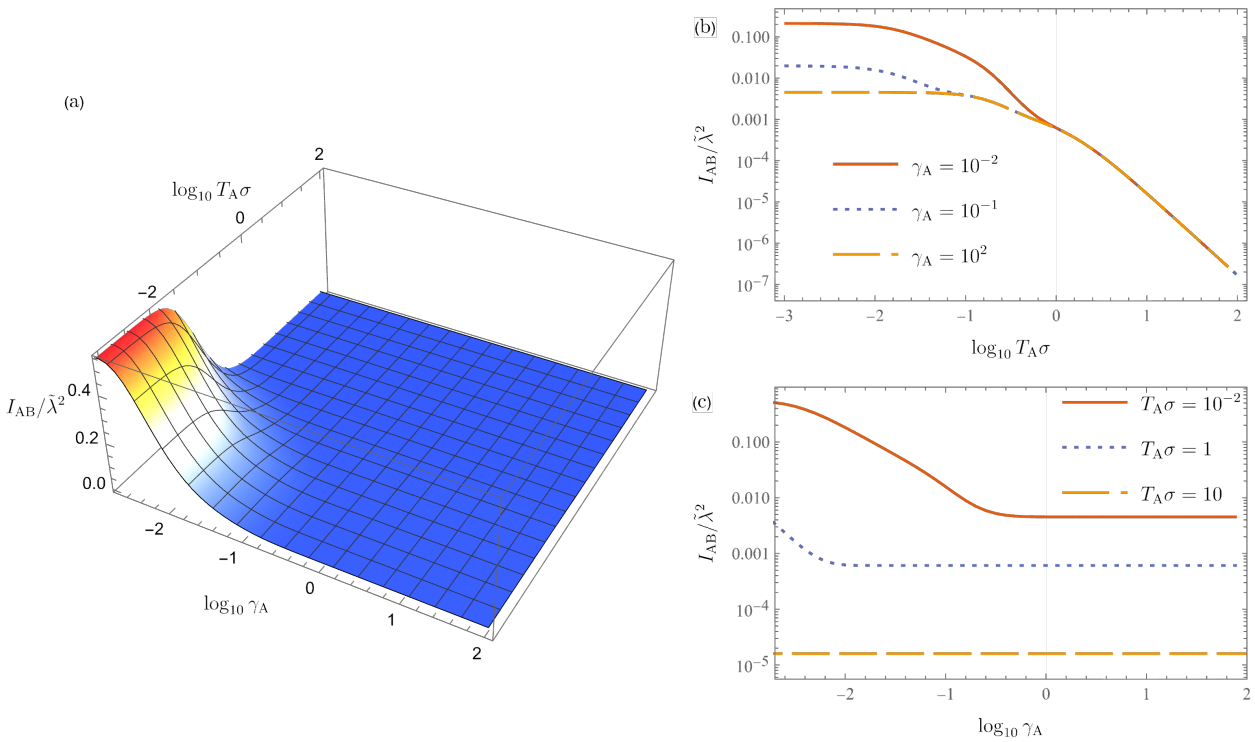


FIG. 3. (a) 3D plot of mutual information $I_{AB}/\tilde{\lambda}^2$ as a function of local temperature T_A and redshift factor γ_A of detector A. Here, $\ell/\sigma = 10, \Omega\sigma = 1$, and $d_{AB}/\sigma = 7$. (b) Slices of (a) at constant γ_A in a logarithmic scale. The curves in the lower temperature show the scenario where static detectors in AdS_3 spacetime without radiation, and the higher temperature regime represents how Unruh and/or Hawking radiations "attack" the detectors. (c) Slices of (a) at constant $T_A\sigma$ in a logarithmic scale. The contribution coming from the black hole can be seen in $\gamma_A \ll 1$ regime. As $\gamma_A \to \infty$, the Hawking effect becomes negligible and only Unruh effect survives.

also [27, 39, 40, 44]), where

$$T_{EDR} = -\frac{\Omega}{\ln \mathcal{R}} \tag{26}$$

with

$$\mathcal{R} = \frac{\mathcal{F}(\Omega)}{\mathcal{F}(-\Omega)}\,, \tag{27}$$

being the excitation-to-de-excitation ratio of the detector. For an accelerating detector in a flat spacetime these effects are respectively referred to as weak and strong anti-Unruh phenomena [45, 46], and will not be present in a situation where an inertial detector is in a thermal bath.

Since there is a range in temperature in which $\mathcal{L}_{AA}/\tilde{\lambda}^2$ decreases, the detector exhibits the weak anti-Hawking effect and the redshift is not involved. Also note that (under the Dirichlet boundary condition) this originates from the BTZ part of the Wightman function, as demonstrated in [38].

Figure 2(b-iii) shows that the off-diagonal term $\mathcal{L}_{AB}/\tilde{\lambda}^2$ asymptotes to 0 as $T_A\sigma \to \infty$. This suggests that it is extreme temperature that inhibits detectors from harvesting mutual information. Hence, the fact that the detectors cannot extract correlations when one of them is at the event horizon [Figs. 1(a), (c)] is purely due to the extremity of the local Hawking radiation there, which is a combination of increasing black hole mass with decreasing d_A so as to ensure constant redshift.

Finally, we plot mutual information I_{AB} as a function of detector A's local temperature, T_A, and the redshift factor, γ_A, in Fig. 3(a). Here we fix $\ell/\sigma = 10$, $d_{AB}/\sigma = 7$, and $\Omega\sigma = 1$. One can observe from Fig. 3(a) that the detectors easily harvest mutual information when the temperature T_A and redshift γ_A are both small. This corresponds to a case where two detectors are located far away ($d_A/\sigma \gg 1$) from a tiny black hole ($r_h/\sigma \ll 1$). On the other hand, high temperature or large redshift factor, which corresponds to $r_h/\sigma \gg 1$ and $d_A/\sigma \ll 1$, suppress the extraction of correlation.

Figure 3(b) depicts slices of Fig. 3(a) with constant γ_A in a logarithmic scale to analyze the relationship of mutual information with the Hawking effect. As the figure indicates, the colder the temperature, the more the correlation harvested, whereas $I_{AB}/\tilde{\lambda}^2 \to 0$ as the temperature gets large. This indicates that the radiation from the black hole acts as noise that inhibits extraction of correlation by the detectors, and this is true no matter what the value of redshift is.

Conversely, Fig. 3(c) exhibits the influence of redshift γ_A while the temperature T_A is fixed. In contrast

to Fig. 3(b), mutual information does not go to 0 as $\gamma_{\rm A} \to \infty$. Instead, it asymptotes to a finite value that is characterized by the temperature $T_{\rm A}$. As we saw in Fig. 2(a-ii) and (a-iii), the BTZ part of $\mathcal{L}_{ij}$ vanishes at large $\gamma_{\rm A}$, leading us to conclude that the asymptotic values in Fig. 3(c) coincide with mutual information harvested by *accelerating* detectors in AdS_3 spacetime with corresponding accelerations that give local temperature $T_{\rm A}$. From these figures, we conclude that the death of mutual information in a black hole spacetime is purely due to Hawking radiation. We have checked that this feature holds for other boundary conditions ($\zeta = 0, -1$).

IV. CONCLUSION

Based on the fact that a vacuum state of a quantum field is entangled and that such correlations contain information about the background spacetime, correlation harvesting protocols are of great interest in relativistic quantum information theory. In this paper, we investigated the harvesting protocol for mutual information with two static UDW detectors in a nonrotating BTZ black hole spacetime.

As shown in Refs. [19, 26, 29, 30], there exists a region, the so-called entanglement shadow, near a black hole where static detectors cannot extract entanglement from the vacuum. It was suggested that the entanglement shadow is a consequence of the Hawking effect and gravitational redshift [19]. Inspired by these results, we have examined the effect of Hawking radiation and gravitational redshift on harvested mutual information $I_{\rm AB}$ between detectors A and B by considering $I_{\rm AB}$ as a function of local temperature $T_{\rm A}$ and redshift factor $\gamma_{\rm A}$ of detector A: $I_{\rm AB} = I_{\rm AB}(T_{\rm A}, \gamma_{\rm A})$. We find that the black hole has a significant effect on the mutual information extracted, with high temperature and extreme redshift preventing the detectors from extracting correlation.

We first confirmed that, unlike entanglement, there is no "mutual information shadow" in agreement with Refs. [26, 30]. Mutual information vanishes only when one of the detectors reaches the event horizon, and this is true for any value of energy gap Ω. We then showed that, by looking at the effects of redshift and Hawking radiation separately, extreme Hawking radiation (and not gravitational redshift) is responsible for the death of mutual information . That is, as the local temperature increases while fixing $\gamma_{\rm A}$, we found $I_{\rm AB} \to 0$.

Remarkably, the death of mutual information at extreme temperature is in contrast to what was found in flat spacetime [31]. Two inertial detectors interacting with a thermal field state in Minkowski spacetime struggle to extract entanglement but easily harvest mutual information as the field temperature increases. Since this result holds for any spacetime dimension, switching functions, and detector shapes [31], the striking distinction between our result from theirs may come from (i) the existence of curvature, and/or (ii) the effects of acceleration. Concerning (i), the background spacetime has no curvature in [31] whereas the BTZ spacetime has constant negative curvature. One can check the relevance of curvature by putting inertial detectors in AdS_3 spacetime, which we do not investigate in this paper. Concerning (ii), our static detectors in BTZ spacetime are constantly accelerating away from a black hole, whereas the previous study considered inertial detectors [31]. A single detector can exhibit the anti-Unruh effect when accelerating, but not if it is inertial in a thermal bath [46]. In the context of entanglement harvesting, detectors accelerating in a vacuum state and inertial in a thermal state can be distinguished [23, 25]. It would be interesting to compare mutual information in scenarios with and without acceleration in the same spacetime.

ACKNOWLEDGMENTS

This work was supported in part by the Natural Sciences and Engineering Research Council of Canada and by Asian Office of Aerospace Research and Development Grant No. FA2386-19-1-4077.

Appendix A: DERIVATION OF $\mathcal{L}_{\rm AB}$

Consider static detectors on the same axis originating at the center of the black hole (i.e., $\Delta\phi = 0$). Assuming that both detectors switch at the same time, we have

$$\mathcal{L}_{\rm AB} = \lambda^2 \int_{\mathbb{R}} {\rm d}\tau_{\rm A} \int_{\mathbb{R}} {\rm d}\tau_{\rm B}\, e^{-\tau_{\rm A}^2/2\sigma^2} e^{-\tau_{\rm B}^2/2\sigma^2} e^{-{\rm i}\Omega(\tau_{\rm A}-\tau_{\rm B})} W_{\rm BTZ}(\mathsf{x}_{\rm A}(\tau_{\rm A}), \mathsf{x}_{\rm B}(\tau_{\rm B})), \tag{A1}$$

where

$$W_{\rm BTZ}(\mathsf{x}_{\rm A}(\tau_{\rm A}), \mathsf{x}_{\rm B}(\tau_{\rm B})) = \frac{1}{4\pi\sqrt{2}\ell} \sum_{n=-\infty}^{\infty} \left[\frac{1}{\sqrt{\sigma_\epsilon(\mathsf{x}_{\rm A}, \Gamma^n \mathsf{x}_{\rm B})}} - \frac{\zeta}{\sqrt{\sigma_\epsilon(\mathsf{x}_{\rm A}, \Gamma^n \mathsf{x}_{\rm B}) + 2}} \right], \tag{A2}$$

$$\sigma_\epsilon(\mathsf{x}_{\rm A}, \Gamma^n \mathsf{x}_{\rm B}) = \frac{r_{\rm A} r_{\rm B}}{r_{\rm h}^2} \cosh\left(\frac{r_{\rm h}}{\ell} 2\pi n\right) - 1 - \frac{\sqrt{(r_{\rm A}^2 - r_{\rm h}^2)(r_{\rm B}^2 - r_{\rm h}^2)}}{r_{\rm h}^2} \cosh\left[\frac{r_{\rm h}}{\ell^2}\left(\frac{\tau_{\rm A}}{\gamma_{\rm A}} - \frac{\tau_{\rm B}}{\gamma_{\rm B}}\right) - {\rm i}\epsilon\right], \tag{A3}$$

where we used $t_j = \tau_j/\gamma_j$. Then $\mathcal{L}_{\mathrm{AB}}$ becomes

$$\mathcal{L}_{\mathrm{AB}} = \frac{\lambda^2}{4\pi\sqrt{2}\ell} \sum_{n=-\infty}^{\infty} \int_{\mathbb{R}} \mathrm{d}\tau_{\mathrm{A}} \int_{\mathbb{R}} \mathrm{d}\tau_{\mathrm{B}}\, e^{-\tau_{\mathrm{A}}^2/2\sigma^2} e^{-\tau_{\mathrm{B}}^2/2\sigma^2} e^{-\mathrm{i}\Omega(\tau_{\mathrm{A}}-\tau_{\mathrm{B}})} \left[\frac{1}{\rho^-(\mathsf{x}_{\mathrm{A}}, \Gamma^n \mathsf{x}_{\mathrm{B}})} - \frac{\zeta}{\rho^+(\mathsf{x}_{\mathrm{A}}, \Gamma^n \mathsf{x}_{\mathrm{B}})}\right], \tag{A4}$$

where

$$\rho^{\pm}(\mathsf{x}_{\mathrm{A}}, \Gamma^n \mathsf{x}_{\mathrm{B}}) \coloneqq \sqrt{\frac{r_{\mathrm{A}} r_{\mathrm{B}}}{r_{\mathrm{h}}^2} \cosh\left[\frac{r_{\mathrm{h}}}{\ell} 2\pi n\right] \pm 1 - \frac{\ell^2 \gamma_{\mathrm{A}} \gamma_{\mathrm{B}}}{r_{\mathrm{h}}^2} \cosh\left[\frac{r_{\mathrm{h}}}{\ell^2}\left(\frac{\tau_{\mathrm{A}}}{\gamma_{\mathrm{A}}} - \frac{\tau_{\mathrm{B}}}{\gamma_{\mathrm{B}}}\right) - \mathrm{i}\epsilon\right]} \tag{A5}$$

$$= \frac{\ell\sqrt{\gamma_{\mathrm{A}}\gamma_{\mathrm{B}}}}{r_{\mathrm{h}}} \sqrt{\cosh \alpha^{\pm}_{\mathrm{AB},\, n} - \cosh\left[\frac{r_{\mathrm{h}}}{\ell^2}\left(\frac{\tau_{\mathrm{A}}}{\gamma_{\mathrm{A}}} - \frac{\tau_{\mathrm{B}}}{\gamma_{\mathrm{B}}}\right) - \mathrm{i}\epsilon\right]}, \tag{A6}$$

and

$$\alpha^{\pm}_{\mathrm{AB},\, n} \coloneqq \operatorname{arccosh}\left[\frac{r_{\mathrm{h}}^2}{\ell^2 \gamma_{\mathrm{A}} \gamma_{\mathrm{B}}}\left(\frac{r_{\mathrm{A}} r_{\mathrm{B}}}{r_{\mathrm{h}}^2} \cosh\left[\frac{r_{\mathrm{h}}}{\ell} 2\pi n\right] \pm 1\right)\right]. \tag{A7}$$

Let us change the variables τ_{A} and τ_{B} to t_{A} and t_{B}, respectively, by the transformation $t_j \coloneqq \tau_j/\gamma_j$.

$$\mathcal{L}_{\mathrm{AB}} = \frac{\lambda^2 \gamma_{\mathrm{A}} \gamma_{\mathrm{B}}}{4\pi\sqrt{2}\ell} \sum_{n=-\infty}^{\infty} \int_{\mathbb{R}} \mathrm{d}t_{\mathrm{A}} \mathrm{d}t_{\mathrm{B}}\, e^{-\gamma_{\mathrm{A}}^2 t_{\mathrm{A}}^2/2\sigma^2} e^{-\gamma_{\mathrm{B}}^2 t_{\mathrm{B}}^2/2\sigma^2} e^{-\mathrm{i}\Omega(\gamma_{\mathrm{A}} t_{\mathrm{A}} - \gamma_{\mathrm{B}} t_{\mathrm{B}})} \left[\frac{1}{\rho^-(t_{\mathrm{A}}, t_{\mathrm{B}})} - \frac{\zeta}{\rho^+(t_{\mathrm{A}}, t_{\mathrm{B}})}\right], \tag{A8}$$

where

$$\rho^{\pm}(t_{\mathrm{A}}, t_{\mathrm{B}}) \coloneqq \frac{\ell\sqrt{\gamma_{\mathrm{A}}\gamma_{\mathrm{B}}}}{r_{\mathrm{h}}} \sqrt{\cosh \alpha^{\pm}_{\mathrm{AB},\, n} - \cosh\left[\frac{r_{\mathrm{h}}}{\ell^2}\left(t_{\mathrm{A}} - t_{\mathrm{B}}\right) - \mathrm{i}\epsilon\right]}. \tag{A9}$$

Further changing coordinates $u \coloneqq t_{\mathrm{A}} - t_{\mathrm{B}}, s \coloneqq t_{\mathrm{A}} + t_{\mathrm{B}}$, the corresponding Jacobian determinant is $J = 1/2$, and so $\mathcal{L}_{\mathrm{AB}}$ becomes

$$\mathcal{L}_{\mathrm{AB}} = \frac{\lambda^2 \gamma_{\mathrm{A}} \gamma_{\mathrm{B}}}{8\pi\sqrt{2}\ell} \sum_{n=-\infty}^{\infty} \int_{\mathbb{R}} \mathrm{d}u\, e^{-(\gamma_{\mathrm{A}}^2+\gamma_{\mathrm{B}}^2)u^2/8\sigma^2} e^{-\mathrm{i}\Omega(\gamma_{\mathrm{A}}+\gamma_{\mathrm{B}})u/2} \left[\frac{1}{\rho^-(u)} - \frac{\zeta}{\rho^+(u)}\right]$$
$$\times \int_{\mathbb{R}} \mathrm{d}s\, e^{-(\gamma_{\mathrm{A}}^2+\gamma_{\mathrm{B}}^2)s^2/8\sigma^2} e^{-(\gamma_{\mathrm{A}}^2-\gamma_{\mathrm{B}}^2)us/4\sigma^2} e^{-\mathrm{i}\Omega(\gamma_{\mathrm{A}}-\gamma_{\mathrm{B}})s/2} \tag{A10}$$

$$= \frac{\lambda^2 \sigma \gamma_{\mathrm{A}} \gamma_{\mathrm{B}}}{4\ell\sqrt{\pi}\sqrt{\gamma_{\mathrm{A}}^2+\gamma_{\mathrm{B}}^2}} \exp\left[-\frac{\Omega^2\sigma^2(\gamma_{\mathrm{A}}-\gamma_{\mathrm{B}})^2}{2(\gamma_{\mathrm{A}}^2+\gamma_{\mathrm{B}}^2)}\right] \sum_{n=-\infty}^{\infty} \int_{\mathbb{R}} \mathrm{d}u\, e^{-au^2} e^{-\mathrm{i}\beta u} \left[\frac{1}{\rho^-(u)} - \frac{\zeta}{\rho^+(u)}\right] \tag{A11}$$

$$= 2K \sum_{n=-\infty}^{\infty} \operatorname{Re} \int_0^{\infty} \mathrm{d}x\, e^{-ax^2} e^{-\mathrm{i}\beta x} \left[\frac{1}{\sqrt{\cosh \alpha^-_{\mathrm{AB},\, n} - \cosh x}} - \frac{\zeta}{\sqrt{\cosh \alpha^+_{\mathrm{AB},\, n} - \cosh x}}\right], \tag{A12}$$

where

$$a \coloneqq \frac{\gamma_{\mathrm{A}}^2 \gamma_{\mathrm{B}}^2}{2\sigma^2(\gamma_{\mathrm{A}}^2+\gamma_{\mathrm{B}}^2)} \frac{\ell^4}{r_{\mathrm{h}}^2}, \tag{A13a}$$

$$\beta \coloneqq \frac{\gamma_{\mathrm{A}}\gamma_{\mathrm{B}}(\gamma_{\mathrm{A}}+\gamma_{\mathrm{B}})}{\gamma_{\mathrm{A}}^2+\gamma_{\mathrm{B}}^2} \frac{\ell^2}{r_{\mathrm{h}}} \Omega\,, \tag{A13b}$$

$$K \coloneqq \frac{\lambda^2 \sigma \sqrt{\gamma_{\mathrm{A}}\gamma_{\mathrm{B}}}}{4\sqrt{\pi}\sqrt{\gamma_{\mathrm{A}}^2+\gamma_{\mathrm{B}}^2}} \exp\left[-\frac{\Omega^2\sigma^2(\gamma_{\mathrm{A}}-\gamma_{\mathrm{B}})^2}{2(\gamma_{\mathrm{A}}^2+\gamma_{\mathrm{B}}^2)}\right]. \tag{A13c}$$

Although the integrand in Eq. (A12) does not have a pole, one needs to be careful about the branch cuts as shown in Fig. 4. Equation (A12) can be obtained by evaluating along L_1, C_ρ, and L_2 in the limit $R \to \infty$ and $\rho \to 0$, where ρ is the radius of the semicircle around the branch point.

Let us choose a contour in the complex plane and use the Cauchy integral theorem. To do so, consider a complex integral of Eq. (A12):

$$\oint_C \mathrm{d}z\, e^{-az^2} e^{-\mathrm{i}\beta z} \left[\frac{1}{\sqrt{\cosh \alpha^-_{\mathrm{AB},\, n} - \cosh z}} - \frac{\zeta}{\sqrt{\cosh \alpha^+_{\mathrm{AB},\, n} - \cosh z}}\right]. \tag{A14}$$

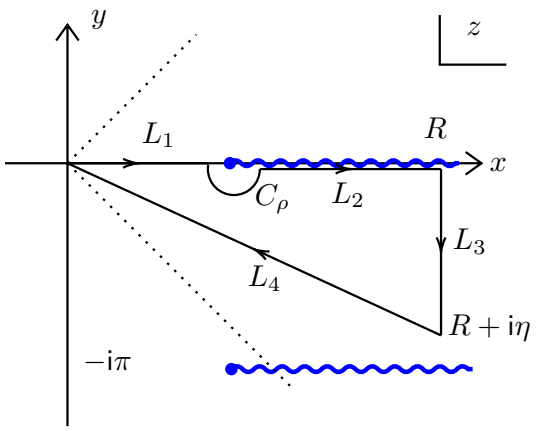


FIG. 4. Contour in a complex plane. Blue wiggly lines are the branch cuts and the contour is chosen so that the integral converges when $\Omega > 0$. The dotted lines represent $y = \pm x$, and the contour must be inside of this region.

Assuming $\Omega > 0$, the integral (A14) converges if $|e^{-az^2}e^{-\mathrm{i}\beta z}| = e^{-a(x^2-y^2)}e^{\beta y} < 1$, where we used $z = x + \mathrm{i}y$, and so the contour C should be in $y < 0$ and $-x \le y \le x$. From this, we choose the contour $C = L_1 C_\rho L_2 L_3 L_4$ as shown in Fig. 4 and by making use of the Cauchy integral theorem with the fact that $\lim_{R\to\infty}\int_{L_3} = 0$, Eq. (A12) becomes an integral along L_4^{-1}:

$$\mathcal{L}_{\mathrm{AB}} = 2K\sum_{n=-\infty}^{\infty}\lim_{R\to\infty}\mathrm{Re}\int_0^{R+\mathrm{i}\eta}\mathrm{d}z\, e^{-az^2}e^{-\mathrm{i}\beta z}\left[\frac{1}{\sqrt{\cosh\alpha^-_{\mathrm{AB},\,n}-\cosh z}}-\frac{\zeta}{\sqrt{\cosh\alpha^+_{\mathrm{AB},\,n}-\cosh z}}\right], \tag{A15}$$

where $\eta \in (-\pi, 0)$ and $\Omega > 0$; this is the expression we compute numerically.

For $\mathcal{L}_{\mathrm{AA}}$ and $\mathcal{L}_{\mathrm{BB}}$, they are known to be [19]

$$\begin{aligned}\mathcal{L}_{\mathrm{DD}} = {}& \frac{\lambda^2\sigma^2}{2}\int_{\mathbb{R}}\mathrm{d}x\,\frac{e^{-\sigma^2(x-\Omega)^2}}{e^{x/T_{\mathrm{D}}}+1}-\zeta\frac{\lambda^2\sigma}{2\sqrt{2\pi}}\mathrm{Re}\int_0^\infty\mathrm{d}x\,\frac{e^{-a_{\mathrm{D}}x^2}e^{-\mathrm{i}\beta_{\mathrm{D}}x}}{\sqrt{\cosh\alpha^+_{\mathrm{D},0}-\cosh x}}\\ &+\frac{\lambda^2\sigma}{\sqrt{2\pi}}\sum_{n=1}^{\infty}\mathrm{Re}\int_0^\infty\mathrm{d}x\,e^{-a_{\mathrm{D}}x^2}e^{-\mathrm{i}\beta_{\mathrm{D}}x}\left(\frac{1}{\sqrt{\cosh\alpha^-_{\mathrm{D},\,n}-\cosh x}}-\frac{\zeta}{\sqrt{\cosh\alpha^+_{\mathrm{D},\,n}-\cosh x}}\right),\end{aligned} \tag{A16}$$

where $T_{\mathrm{D}} = r_{\mathrm{h}}/2\pi\ell^2\gamma_{\mathrm{D}}$ is the local temperature at $r = r_{\mathrm{D}}$ and

$$a_{\mathrm{D}} \coloneqq \frac{\ell^4\gamma_{\mathrm{D}}^2}{4\sigma^2 r_{\mathrm{h}}^2},\ \beta_{\mathrm{D}} \coloneqq \frac{\ell^2\gamma_{\mathrm{D}}\Omega}{r_{\mathrm{h}}}, \tag{A17}$$

$$\alpha^{\pm}_{\mathrm{D},\,n} \coloneqq \mathrm{arccosh}\left[\frac{r_{\mathrm{h}}^2}{\gamma_{\mathrm{D}}^2\ell^2}\left(\frac{r^2}{r_{\mathrm{h}}^2}\cosh\left[\frac{r_{\mathrm{h}}}{\ell}2\pi n\right]\pm 1\right)\right]. \tag{A18}$$

The first two terms, which correspond to $n = 0$, are the so-called AdS-Rindler terms and the last term ($n \neq 0$) is known as the BTZ term. The second and third integrals in (A16) also have the same branch cut subtlety, but can be treated in the same manner as for $\mathcal{L}_{\mathrm{AB}}$.

[1] W. G. Unruh, Notes on black-hole evaporation, Phys. Rev. D **14**, 870 (1976).

[2] B. S. DeWitt, Quantum gravity: The new synthesis, in *General Relativity: An Einstein Centenary Survey*, edited by S. W. Hawking and W. Israel (1979) pp. 680–745.

[3] P. M. Alsing and G. J. Milburn, Teleportation with a uniformly accelerated partner, Phys. Rev. Lett. **91**, 180404 (2003).

[4] A. G. S. Landulfo and G. E. A. Matsas, Sudden death

of entanglement and teleportation fidelity loss via the Unruh effect, Phys. Rev. A **80**, 032315 (2009).
[5] M. Cliche and A. Kempf, Relativistic quantum channel of communication through field quanta, Phys. Rev. A **81**, 012330 (2010).
[6] R. H. Jonsson, Quantum signaling in relativistic motion and across acceleration horizons, Journal of Physics A: Mathematical and Theoretical **50**, 355401 (2017).
[7] A. G. S. Landulfo, Nonperturbative approach to relativistic quantum communication channels, Phys. Rev. D **93**, 104019 (2016).
[8] P. Simidzija, A. Ahmadzadegan, A. Kempf, and E. Martín-Martínez, Transmission of quantum information through quantum fields, Phys. Rev. D **101**, 036014 (2020).
[9] I. Fuentes-Schuller and R. B. Mann, Alice falls into a black hole: Entanglement in noninertial frames, Phys. Rev. Lett. **95**, 120404 (2005).
[10] P. M. Alsing, I. Fuentes-Schuller, R. B. Mann, and T. E. Tessier, Entanglement of dirac fields in noninertial frames, Phys. Rev. A **74**, 032326 (2006).
[11] A. Valentini, Non-local correlations in quantum electrodynamics, Phys. Lett. **153A**, 321 (1991).
[12] B. Reznik, Entanglement from the vacuum, Found. Phys. **33**, 167 (2003).
[13] B. Reznik, A. Retzker, and J. Silman, Violating Bell's inequalities in vacuum, Phys. Rev. A **71**, 042104 (2005).
[14] S. J. Summers and R. Werner, The vacuum violates Bell's inequalities, Phys. Lett. **110A**, 257 (1985).
[15] S. J. Summers and R. Werner, Bell's inequalities and quantum field theory. i. general setting, J. Math. Phys. (N.Y.) **28**, 2440 (1987).
[16] A. Pozas-Kerstjens and E. Martín-Martínez, Harvesting correlations from the quantum vacuum, Phys. Rev. D **92**, 064042 (2015).
[17] E. Martín-Martínez, A. R. H. Smith, and D. R. Terno, Spacetime structure and vacuum entanglement, Phys. Rev. D **93**, 044001 (2016).
[18] S. Kukita and Y. Nambu, Harvesting large scale entanglement in de Sitter space with multiple detectors, Entropy **19**, 449 (2017).
[19] L. J. Henderson, R. A. Hennigar, R. B. Mann, A. R. H. Smith, and J. Zhang, Harvesting entanglement from the black hole vacuum, Classical Quantum Gravity **35**, 21LT02 (2018).
[20] K. K. Ng, R. B. Mann, and E. Martín-Martínez, Unruh-DeWitt detectors and entanglement: The anti–de Sitter space, Phys. Rev. D **98**, 125005 (2018).
[21] W. Cong, C. Qian, M. R. Good, and R. B. Mann, Effects of horizons on entanglement harvesting, J. High Energy Phys. **10** (2020), 67.
[22] F. Gray, D. Kubizňák, T. May, S. Timmerman, and E. Tjoa, Quantum imprints of gravitational shockwaves, J. High Energy Phys. **11** (2021), 054.
[23] G. Salton, R. B. Mann, and N. C. Menicucci, Acceleration-assisted entanglement harvesting and rangefinding, New J. Phys. **17**, 035001 (2015).
[24] J. Foo, S. Onoe, and M. Zych, Unruh-dewitt detectors in quantum superpositions of trajectories, Phys. Rev. D **102**, 085013 (2020).
[25] Z. Liu, J. Zhang, R. B. Mann, and H. Yu, Does acceleration assist entanglement harvesting?, Phys. Rev. D **105**, 085012 (2022), arXiv:2111.04392 [quant-ph].
[26] E. Tjoa and R. B. Mann, Harvesting correlations in Schwarzschild and collapsing shell spacetimes, J. High Energy Phys. **08** (2020), 155.
[27] L. d. S. Campos and C. Dappiaggi, Ground and thermal states for the klein-gordon field on a massless hyperbolic black hole with applications to the anti-hawking effect, Phys. Rev. D **103**, 025021 (2021).
[28] L. J. Henderson, S. Y. Ding, and R. B. Mann, Entanglement harvesting with a twist, AVS Quantum Sci. **4**, 014402 (2022), arXiv:2201.11130 [quant-ph].
[29] M. P. G. Robbins, L. J. Henderson, and R. B. Mann, Entanglement amplification from rotating black holes, Classical Quantum Gravity **39**, 02LT01 (2022).
[30] K. Gallock-Yoshimura, E. Tjoa, and R. B. Mann, Harvesting entanglement with detectors freely falling into a black hole, Phys. Rev. D **104**, 025001 (2021).
[31] P. Simidzija and E. Martín-Martínez, Harvesting correlations from thermal and squeezed coherent states, Phys. Rev. D **98**, 085007 (2018).
[32] K. Gallock-Yoshimura and R. B. Mann, Entangled detectors nonperturbatively harvest mutual information, Phys. Rev. D **104**, 125017 (2021).
[33] A. Sahu, I. Melgarejo-Lermas, and E. Martín-Martínez, Sabotaging the harvesting of correlations from quantum fields, Phys. Rev. D **105**, 065011 (2022).
[34] E. Tjoa and E. Martín-Martínez, When entanglement harvesting is not really harvesting, Phys. Rev. D **104**, 125005 (2021).
[35] M. Bañados, C. Teitelboim, and J. Zanelli, Black hole in three-dimensional spacetime, Phys. Rev. Lett. **69**, 1849 (1992).
[36] M. Bañados, M. Henneaux, C. Teitelboim, and J. Zanelli, Geometry of the 2+1 black hole, Phys. Rev. D **48**, 1506 (1993).
[37] G. Lifschytz and M. Ortiz, Scalar field quantization on the (2+1)-dimensional black hole background, Phys. Rev. D **49**, 1929 (1994).
[38] L. J. Henderson, R. A. Hennigar, R. B. Mann, A. R. Smith, and J. Zhang, Anti-hawking phenomena, Physics Letters B **809**, 135732 (2020).
[39] L. de Souza Campos and C. Dappiaggi, The anti-hawking effect on a btz black hole with robin boundary conditions, Physics Letters B **816**, 136198 (2021).
[40] M. P. G. Robbins and R. B. Mann, Anti-hawking phenomena around a rotating btz black hole (2021).
[41] D. Jennings, On the response of a particle detector in Anti-de Sitter spacetime, Class. Quant. Grav. **27**, 205005 (2010), arXiv:1008.2165 [gr-qc].
[42] E. Martín-Martínez and P. Rodriguez-Lopez, Relativistic quantum optics: The relativistic invariance of the light-matter interaction models, Phys. Rev. D **97**, 105026 (2018).
[43] E. Martín-Martínez, T. R. Perche, and B. de S. L. Torres, General relativistic quantum optics: Finite-size particle detector models in curved spacetimes, Phys. Rev. D **101**, 045017 (2020).
[44] A. Conroy and P. Taylor, Response of an unruh-dewitt detector near an extremal black hole, Phys. Rev. D **105**, 085001 (2022).
[45] W. Brenna, R. B. Mann, and E. Martín-Martínez, Anti-Unruh phenomena, Physics Letters B **757**, 307 (2016).
[46] L. J. Garay, E. Martín-Martínez, and J. de Ramón, Thermalization of particle detectors: The Unruh effect and its reverse, Phys. Rev. D **94**, 104048 (2016).